JOC The Journal of Organic Chemistry

Article

pubs.acs.org/joc

Mechanism of Synergistic Cu(II)/Cu(I)-Mediated Alkyne Coupling: Dinuclear 1,2-Reductive Elimination after Minimum Energy Crossing Point

Xiaotian Qi,[†,§] Ruopeng Bai,[‡,§] Lei Zhu,[†] Rui Jin,[†] Aiwen Lei,*[,‡] and Yu Lan*[,†]

[†]School of Chemistry and Chemical Engineering, Chongqing University, Chongqing 400030, People's Republic of China

[‡]College of Chemistry and Molecular Sciences, Wuhan University, Wuhan 430072, Hubei, People's Republic of China

Supporting Information

ABSTRACT: An in-depth theoretical study of synergistic Cu(II)/Cu(I)-mediated alkyne coupling was performed to reveal the detailed mechanism for C−C bond formation, which proceeded via an unusual dinuclear 1,2-reductive elimination. Because the reactant for dinuclear 1,2-reductive elimination was calculated to be triplet while the products were singlet, the minimum energy crossing point (MECP) was introduced to the Cu/TMEDA/alkyne system to clarify the spin crossing between triplet state and singlet state potential energy surfaces. Computational results suggest that C−H bond cleavage solely catalyzed by the Cu(I) cation is the rate-determining step of this reaction and Cu(II)-mediated dinuclear 1,2-reductive elimination after the MECP is a facile process. These conclusions are in good agreement with our previous experimental results.

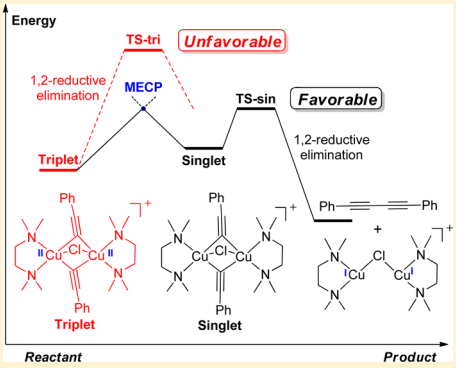

INTRODUCTION

The development of Cu-catalyzed or -mediated coupling reactions has been studied for more than a century, since the pioneering work of Ullmann,[1] Goldberg,[2] and Hurtley[3] in modern Cu chemistry.[4] Cu catalysis is well accepted as a practical and efficient method for the synthesis of various natural products, medicinal molecules, and organic functional materials;[5] for example, the Glaser−Hay[6] and Sonogashira[7] coupling reactions, which use Cu salts to catalyze alkyne coupling, have been widely used for the construction of internal alkynes and diynes.[8] However, most research on these reactions is devoted to synthetic methodology,[9] and more attention needs to be paid to the mechanistic study of Cu/alkyne chemistry.[10]

Generally, Cu-catalyzed or -mediated alkynes coupling reactions proceed through C−H activation of alkynes, which generates a Cu acetylide, followed by reductive elimination from a dinuclear Cu(II) acetylide to give a coupling product.[11] Our previous research using in situ X-ray absorption spectroscopy (XAS) and EPR spectroscopy provided solid evidence for the reduction of $(TMEDA)CuCl_2$ to $[(TMEDA)CuCl]_2$ by terminal alkynes (Scheme 1a).[11c] A plausible inner-sphere electron-transfer process was proposed to clarify the formation of the C−C single bond. Furthermore, in situ Raman spectroscopic studies of synergistic Cu(II)/Cu(I)-mediated terminal alkyne homocoupling (Scheme 1b) showed that Cu(I) rather than Cu(II) participated in the rate-determining step, and it was deduced that Cu(II) acted as oxidant in the C−C bond-construction step.[11a] These investigations provided oxidation state and structural information on Cu intermediates in Cu/TMEDA/alkyne system. However, the detailed mechanism in the Cu/TMEDA/alkyne system still remains unclear and needs to be clarified, especially the reductive elimination process.[12]

Scheme 1. (a) Reduction of $(TMEDA)CuCl_2$ to $[(TMEDA)CuCl]_2$ Using Phenylacetylene, Observed by in Situ XAS and EPR. (b) Synergistic Cu(II)/Cu(I)-Mediated Phenylacetylene Homocoupling Reaction

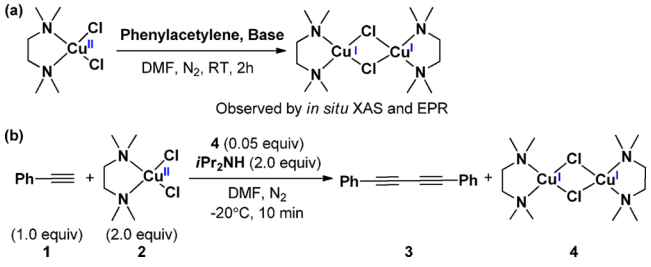

Unlike well-known 1,1-reductive eliminations occurring from mononuclear complexes,[13] the C−C bond formation here is thought to be achieved via an unusual intramolecular dinuclear 1,2-reductive elimination.[14] Our computational results show that the dinuclear Cu acetylide complex was triplet rather than singlet, whereas the product diyne **3** and $[(TMEDA)CuCl]_2$ dimer **4** were singlet, which indicates that the reductive elimination is a two-state reaction.[15] There might be a crossing point between the triplet and singlet 1,2-reductive elimination

Received: December 10, 2015
Published: January 25, 2016

DOI: 10.1021/acs.joc.5b02797
J. Org. Chem. 2016, 81, 1654−1660

potential energy surfaces.[16] This case is consistent with the two-state reactivity concept proposed by Schwarz and co-workers as the Cu-mediated phenylacetylene coupling reaction involves the spin crossover.[17] Therefore, the actual mechanism of this reaction is determined by the interplay of spin inversion and the respective energy span on both spin surfaces. To clarify the spin-inversion process during C−C bond formation, the minimum energy crossing point (MECP)[18] was introduced to the Cu/TMEDA/alkyne system.

Theoretical calculation is a powerful tool for mechanistic studies in organic chemistry.[19] Relative energies and specific structures of intermediates can be obtained via calculation, even for transient intermediates and the minimum energy crossing points (MECPs), which cannot be monitored using experimental techniques.[20] More importantly, the combination of theoretical calculations and experimental results provides more convincing and comprehensive explanations for reaction mechanisms.[21] Here, density functional theory (DFT) calculations were used to investigate the mechanism of synergistic Cu(II)/Cu(I)-mediated phenylacetylene homocoupling reaction.

COMPUTATIONAL METHODS

All the DFT calculations were carried out with the GAUSSIAN 09 series of programs.[22] The DFT method B3-LYP[23] with a standard 6-31G(d) basis set (SDD[24] basis set for Cu) was used for geometry optimizations. Harmonic vibration frequency calculations were performed for all stationary points to confirm them as a local minima or transition structures and to derive the thermochemical corrections for the enthalpies and free energies. Solvent effects were considered by single-point calculations on the gas-phase stationary points using an SMD continuum solvation model.[25] The newly developed M11-L functional with a 6-311+G(d) basis set (SDD basis set for Cu) was used to calculate the solvation single-point energies to give more accurate energy information.[26] The energies given in this work are M11-L calculated Gibbs free energies in *N*,*N*-dimethylformamide (DMF) unless otherwise noted. As shown below, M11-L-calculated Gibbs free energy $G(\mathrm{DMF})_{\mathrm{M11\text{-}L}}$ is obtained by eq 1, in which $E(\mathrm{DMF})_{\mathrm{M11\text{-}L}}$ is the solvation single-point energy calculated at the M11-L/6-311+G(d) level and $G(\mathrm{gas})_{\mathrm{correction}}$ is the thermochemical corrections calculated in gas phase for the Gibbs free energies:

$$G(\mathrm{DMF})_{\mathrm{M11\text{-}L}} = E(\mathrm{DMF})_{\mathrm{M11\text{-}L}} + G(\mathrm{gas})_{\mathrm{correction}} \quad (1)$$

In addition, the MECP in this work were located with the code developed by Harvey and co-workers at the B3-LYP/6-31G(d) level.[27] The final energies of the MECP are the M11-L/6-311+G(d) (SDD basis set for Cu) calculated Gibbs free energies in DMF. Optimized structures are displayed using CYLview.[28]

RESULTS AND DISCUSSION

Our initial calculation focused on the C−H bond activation step, for which four possible pathways are proposed: (1) C−H activation catalyzed solely by Cu(II); (2) C−H activation catalyzed solely by Cu(I); (3) C−H activation co-catalyzed by Cu(II) and Cu(I); and (4) C−H activation catalyzed by di-Cu(I). All of these possibilities were considered, and the corresponding calculations were performed to obtain the most reliable mechanism.

As shown in Figure 1, (TMEDA)$CuCl_2$ (**2**) was set as the relative zero free energy point for the solely Cu(II)-catalyzed C−H activation potential energy surface. Cleavage of the Cu−Cl bond in complex **2** generates Cu(II) cation **5**; the reaction is endothermic by 5.1 kcal/mol. Subsequent π-coordination of phenylacetylene **1** toward Cu gives intermediate **6** with an energy span of 5.9 kcal/mol, followed by hydrogen bonding

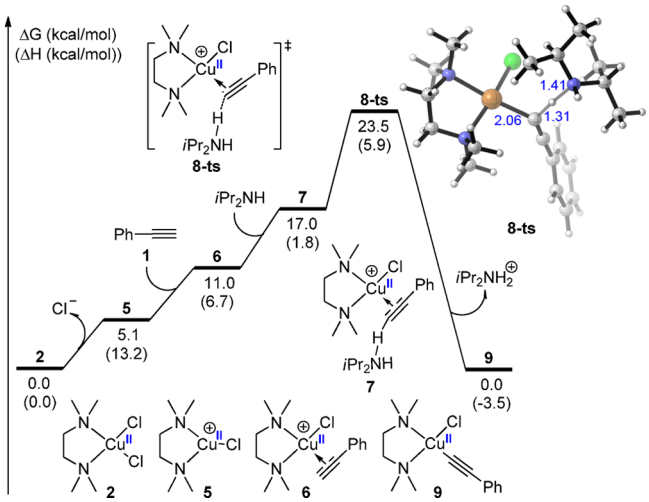

Figure 1. Free energy profile for C−H activation catalyzed solely by Cu(II) and formation of Cu(II) acetylide.

between nitrogen and hydrogen, leading to generation of complex **7** with a relative free energy of 17.0 kcal/mol. Finally, Cu(II) acetylide **9** is generated through deprotonation of transition state **8-ts** with an overall energy span of 23.5 kcal/mol.

Deprotonation solely catalyzed by Cu(I) is shown in Figure 2 (some key structures are given in Figure 3). π-Coordination of the C−C triple bond toward (TMEDA)CuCl (**10**) generates intermediate **11**. Deprotonation then occurs via transition state **13-ts** from hydrogen-bonded intermediate **12**, generating Cu(I)−ate complex **14**. The activation energy is 23.6 kcal/mol, which is nearly equal that in the Cu(II)-catalyzed pathway. Alternatively, deprotonation could take place through a mechanism catalyzed by the Cu(I) cation. As shown in the free energy profile (shown in blue), Cu−Cl bond breakage in complex **11** occurs through transition state **15-ts**; the activation free energy is 3.0 kcal/mol. The formation of Cu(I) cation **16** is exothermic by 3.3 kcal/mol, which indicates that the coordinating ability of phenylacetylene toward the Cu(I) cation is stronger than that of chloride ion. Subsequent C−H bond cleavage could be achieved via transition state **18-ts** with an activation energy of 19.1 kcal/mol, which is 4.5 kcal/mol lower than that of the electroneutral Cu(I)-catalyzed pathway.

The generated Cu(I) acetylide **19** could then combine with (TMEDA)$CuCl_2$ (**2**) and form the dinuclear Cu complex **20**, which contains a chloride-bridging bond. Through a four-membered cyclic transmetalation transition state **21-ts**, the alkynyl group could migrate from Cu(I) to Cu(II), thereby generating the Cu(II) acetylide **9** and (TMEDA)CuCl **10**. The activation energy for transmetalation is only 9.3 kcal/mol. Consequently, as the rate-determining step of this free energy profile, the deprotonation process catalyzed by Cu(I) cation is more favorable than the electrically neutral Cu(I) catalysis mechanism and the Cu(II) sole catalysis mechanism.

In addition to the pathways catalyzed by Cu(II) or Cu(I), the collaboration between Cu(II) and Cu(I) in C−H activation is also taken into account (Figure 4). Combination of alkyne-coordinated Cu(II) complex **6** with (TMEDA)CuCl (**10**) through π bond coordination could form a dinuclear Cu intermediate **22**, with an energy span of 4.9 kcal/mol. The optimized structure of **22** suggests that Cu(II) and Cu(I) are connected by the p orbital vertical to the benzene ring. The

DOI: 10.1021/acs.joc.5b02797
J. Org. Chem. 2016, 81, 1654−1660

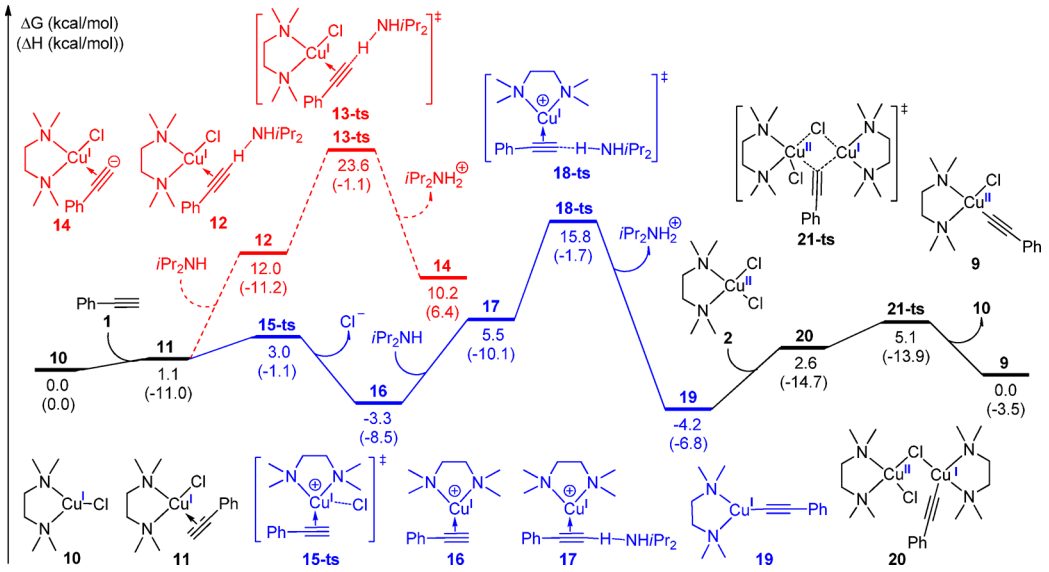

Figure 2. Free energy profile for C−H bond activation catalyzed solely by Cu(I) and formation of Cu(II) acetylide.

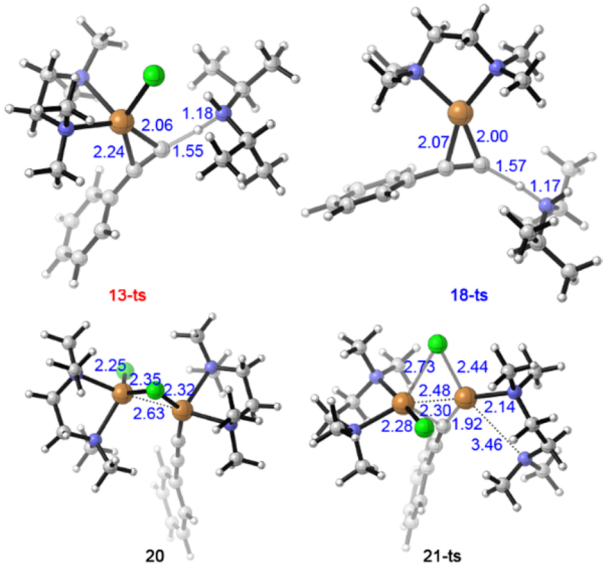

Figure 3. Optimized structures of transition states **13-ts**, **18-ts**, and **21-ts** and dinuclear Cu complex **20**.

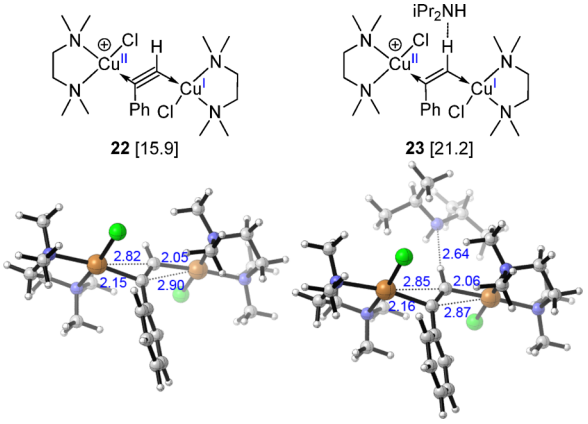

Figure 4. Optimized intermediates in Cu(II)/Cu(I)-cocatalyzed C−H activation pathway. The values in square brackets are the free energies relative to that of alkyne-coordinated Cu(II) cation **6**.

relative free energy and structural information for the corresponding hydrogen-bonded complex **23** are also given. Although the deprotonation transition state could not be located, the relative free energy of complex **23** was calculated to be 21.2 kcal/mol, which is 4.2 kcal/mol higher than that of complex **7**. Furthermore, this energy span is already 2.1 kcal/mol higher than the overall energy span in the pathway catalyzed solely by Cu(I). The Cu(II)/(I) cocatalyzed C−H activation pathway is therefore less favorable than the Cu(I) cation catalysis mechanism.

Experiments and calculations both show that the Cu(I) cation has excellent catalytic activity; therefore, the di-Cu(I) catalysis model may be a good alternative mechanism for C−H activation. A chloride-bridged dinuclear Cu(I) intermediate **24** is obtained by the combination of the alkyne-coordinated Cu(I) cation **16** and electroneutral Cu(I) **10** (Figure 5), whereas a similar C−C triple bond bridged structure as complex **22** is not located. Structural analysis of complex **24** suggests that the alkyne is only π-coordinated to the Cu(I) cation. The bond length of electroneutral Cu(I)−Cl is 2.19 Å, while the cationic Cu(I)−Cl bond length is 2.80 Å, which indicates weak coordination of chloride to the Cu(I) cation. In the

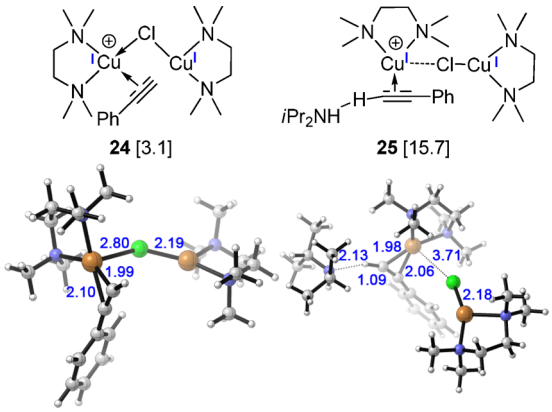

Figure 5. Optimized intermediates in di-Cu(I)-catalyzed C−H activation pathway. The values in square brackets are the free energy relative to alkyne-coordinated Cu(I) cation **16**.

DOI: 10.1021/acs.joc.5b02797
J. Org. Chem. 2016, 81, 1654−1660

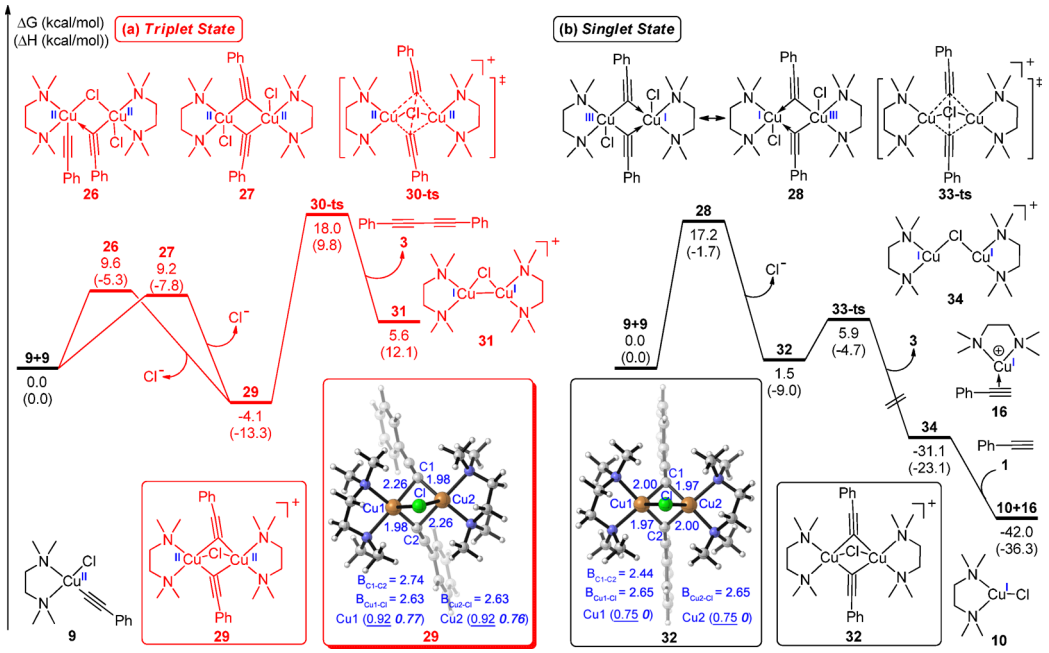

Figure 6. Free energy profiles of triplet state (a) and singlet state (b) 1,2-reductive elimination for the C−C bond formation. The underlined numbers are the NPA charges of copper atoms, followed by numbers in bold italic are the Mulliken spin densities located on each copper.

hydrogen-bonded complex **25**, the cationic Cu(I)−Cl bond is lengthened to 3.71 Å. This distance is so long that there is almost no interaction between the cationic Cu and chloride; therefore, complex **25** is supposed to be unstable. From the energetic point of view, the energy span for the generation of complex **25** from **16** is 19.0 kcal/mol, almost the same as the deprotonation activation energy (19.1 kcal/mol) in the mechanism catalyzed by the Cu(I) cation. The relative free energy of deprotonation transition state would be higher than that of the intermediate; therefore, the di-Cu(I) catalyzed C−H activation pathway can be ruled out, although the structure of the transition state was not obtained.

Subsequent C−C bond formation via 1,2-reductive elimination starts from the dimerization of Cu(II) acetylide **9**, which leads to the generation of a dinuclear Cu(II) acetylide complex. Because the outer electronic configuration of Cu(II) is 3d,[9] both triplet (**26** and **27**) and singlet (**28**) dinuclear Cu intermediates were located in the calculation (Figure 6).

Optimized structures in Figure 6a suggest that chloride and alkynyl groups are simultaneously used as the bridging bonds in triplet Cu dimer **26**. The alkynyl groups therein lie in the *cis* position, and the relative free energy of **26** is 9.6 kcal/mol. When the alkynyl groups are located at the *trans* position, a triplet isomer **27** using terminal carbons of alkynes as bridging bonds is formed. The relative free energy is 9.2 kcal/mol. The corresponding singlet structure of **27** is shown as dimer **28** (Figure 6b), although the corresponding singlet structure of **26** cannot be obtained. The singlet Cu dimer **28** has two resonance structures, which are given in Figure 6b. From an energy point of view, the relative free energy of **28** is 17.2 kcal/mol, which is 7.6 and 8.0 kcal/mol higher than that of triplet dimers **26** and **27**, respectively. Consequently, the formation of singlet dinuclear Cu acetylide is unfavorable.[29]

Followed by dissociation of chloride from triplet Cu dimer, **26** or **27** generates a more stable cation intermediate **29**, the relative free energy of which is −4.1 kcal/mol (the dissociation of another chloride is thermodynamically unfavorable, and both of the dissociation transition states are not located; see Figure S3 in the Supporting Information for details). Structural information on **29** is also given. As shown in the CYLview structure, both alkynyl groups and chloride are employed as the bridging bonds, which makes the combination between two Cu atoms stronger than that in **26** or **27** and therefore contributes to the extra stability. In addition, calculated NPA charges of Cu1 and Cu2 in **29** are equal (i.e., 0.92), and the Mulliken spin densities of Cu1 and Cu2 are almost the same (0.77 for Cu1, 0.76 for Cu2). These data imply that (1) the spin state of intermediate **29** is indeed triplet and (2) the coordination environment and electronic property of each Cu in **29** are nearly equivalent.[30]

The free energy profile of the triplet state ends with the 1,2-reductive elimination of **29**. Through transition state **30-ts**, the coupling product **3** and intermediate **31** are generated; activation free energy for this step is 22.1 kcal/mol. The relative free energy of **3** and **31** is 5.6 kcal/mol, which indicates the C−C bond formation process along triplet potential energy surface is endergonic.

On the singlet free energy profile (Figure 6b), analogous dissociation of chloride from **28** leads to the generation of a singlet cationic intermediate **32**. As shown in the CYLview structure of **32**, the Mulliken spin densities on Cu1 and Cu2 are all zero, which confirms the spin state of **32** is truly singlet. Moreover, the bond lengths of Cu1−C1, Cu2−C1, Cu1−C1, and Cu2−C1 in **32** are very close, which is different from those in triplet cation intermediate **29** as the bond lengths of Cu1−C1 and Cu2−C1 therein are 2.26 and 1.98 Å, respectively. This difference reflects the distinction of alkynyl coordination modes in singlet and triplet Cu complexes. Although the relative free energy of **32** is 5.6 kcal/mol higher than that of **29**, the activation free energy of 1,2-reductive elimination via transition state **33-ts** (5.9 kcal/mol) is 16.2 kcal/mol lower than that on triplet free energy profile. The generation of product **3** and singlet intermediate **34** is exergonic by 31.1 kcal/mol. Subsequent coordination of phenylacetylene **1** to Cu(I) cation

DOI: 10.1021/acs.joc.5b02797
J. Org. Chem. 2016, 81, 1654−1660

in 34 can regenerate intermediate **16** and **10**. The comparison between singlet and triplet free energy profile suggests that (1) the dimerization of Cu(II) acetylide **9** prefers to generate a triplet cationic intermediate for reductive elimination, rather than a singlet intermediate, and (2) the 1,2-reductive elimination for C−C bond formation on a singlet free energy profile is more favorable than that on triplet free energy profile, both kinetically and thermodynamically.

However, it is inadequate to simply describe the C−C bond formation process as either a low-spin state pathway or high-spin state pathway because the reactant for 1,2-reductive elimination is proven to be triplet while the products are singlet. Along with the decrease of C−C bond distance, the triplet and singlet potential energy surfaces will cross each other, and a spin transition is assumed to occur at the crossing point. Locating the minimum energy on the hypersurface where the two spin states have the same energy, i.e., the MECP, would therefore provide valuable information for the energy span of C−C bond formation.

In order to describe the emergence of crossing point more clearly, a structure scan along the triplet reductive elimination surface at B3-LYP/6-31G(d) level was carried out. The structure of relatively stable intermediate **29** was employed as the starting point. The distance between two terminal alkynyl carbons (C1 and C2) was chosen as the coordinate. In total, 11 points were indicated on the triplet potential energy curve (Figure 7, red line). Meanwhile, the corresponding singlet

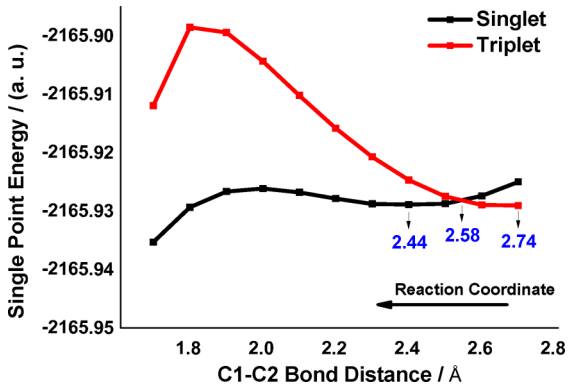

Figure 7. Triplet and singlet potential energy curves obtained by constrained geometry optimizations during C−C bond construction. The distance between carbon C1 and C2 in **29** was chosen as the coordinate. The step size between each point was set to 0.1 Å.

structure of each point was also obtained by constrained geometry optimization (black line). As shown by the red line, the triplet potential energy curve initially increases with the reduction of C1−C2 bond distance and then decreases after the maximum value.

On the other hand, the singlet potential energy curve shows a tendency of decline from the C1−C2 bond distance 2.74 to 2.44 Å. The structure corresponding to 2.44 Å has the local energy minimum, and further optimization of this structure can gain the singlet intermediate **32**. As the C1−C2 bond distance continues to decrease, the singlet curve increases and finally declines after the maximum value. Obviously, these two curves have one crossing point as they intersect with each other at around 2.58 Å.

An accurate structure of the crossing point is located as the minimum energy crossing point **35-MECP**. The CYLview structure shown in Figure 8 suggests that the C1−C2 bond distance in **35-MECP** is 2.64 Å. Through this structure, the

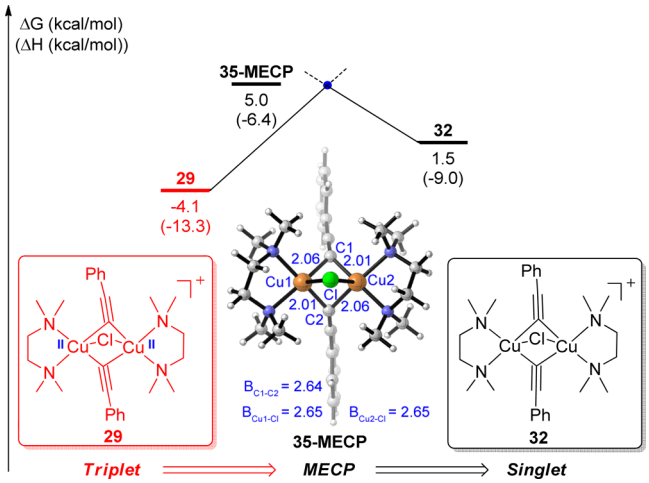

Figure 8. MECP between the triplet and singlet potential energy surfaces.

singlet intermediate **32** can be easily generated from triplet intermediate **29**; the energy span is only 9.1 kcal/mol. Subsequent 1,2-reductive elimination on the singlet potential energy surface via **33-ts** can afford the coupling product **3** (Figure 6b). Consequently, the overall activation free energy for 1,2-reductive elimination is 10.0 kcal/mol, which is 9.1 kcal/mol lower than that in Cu(I) cation catalyzed deprotonation. Furthermore, these data also indicate that the spin crossing between triplet-state and singlet-state potential energy surfaces in this work is a facile process.

On the basis of the above research, a complete reaction pathway for synergistic Cu(II)/Cu(I)-mediated alkyne coupling is given in Scheme 2. The C−H bond activation of alkyne

Scheme 2. Complete Reaction Pathway for Synergistic Cu(II)/Cu(I)-Mediated Alkyne Coupling

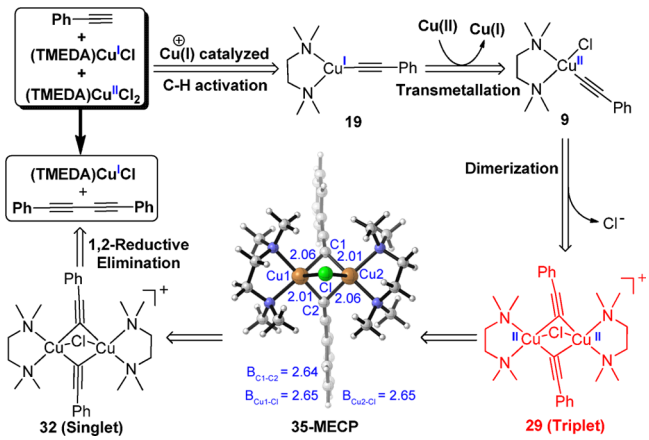

proceeds via Cu(I) cation catalyzed deprotonation, generating Cu(I) acetylide **19**. This process is the rate-determining step, and the activation free energy is 19.1 kcal/mol.[31] Subsequent transmetalation between $(TMEDA)CuCl_2$ and Cu(I) acetylide **19** affords the Cu(II) acetylide **9**. The dimerization of **9** and the dissociation of chloride ion forms a triplet cationic intermediate **29**. The corresponding singlet cationic intermediate **32** is

DOI: 10.1021/acs.joc.5b02797
J. Org. Chem. 2016, 81, 1654−1660

formed by the spin-flip process via **35-MECP**. Finally, the 1,2-reductive elimination on the singlet potential energy surface generates the alkyne homocoupling product, thereby finishing the catalytic cycle.

CONCLUSION

In summary, DFT calculations were performed to investigate synergistic Cu(II)/Cu(I)-catalyzed phenylacetylene homocoupling to highlight the 1,2-reductive elimination for C−C bond formation. As the reactant for 1,2-reductive elimination is demonstrated to be triplet and products are singlet, the MECP is introduced to clarify the spin inversion process. According to the computational results, the conclusion could be drawn that C−H bond cleavage catalyzed by the Cu(I) cation is the rate-determining step of this reaction, and the C−C bond formation accomplished by Cu(II)-mediated 1,2-reductive elimination after the MECP is a fast process. The theoretical results are consistent with our previous experimental results. We believe that the introduction of an MECP into the Cu/TMEDA/alkyne system will bring new insights for Cu-catalyzed transformations.

ASSOCIATED CONTENT

Supporting Information

The Supporting Information is available free of charge on the ACS Publications website at DOI: 10.1021/acs.joc.5b02797.

Cartesian coordinates and energies of all reported structures and full authorship of Gaussian 09 (PDF)

AUTHOR INFORMATION

Corresponding Authors

*E-mail: aiwenlei@whu.edu.cn.

*E-mail: lanyu@cqu.edu.cn.

Author Contributions

§X.Q. and R.B. contributed equally to this work.

Notes

The authors declare no competing financial interest.

ACKNOWLEDGMENTS

This work was supported by the National Natural Science Foundation of China (Grant Nos. 21372266, 21390400, 21272180, 21302148, and 51302327) and the Foundation of 100Young Chongqing University (Project No. 0903005203191). We are also thankful for the project (No. 106112015CDJZR228806) supported by the Fundamental Research Funds for the Central Universities (Chongqing University). We are especially grateful to Prof. Harvey for providing us the program.

REFERENCES

(1) (a) Ullmann, F. *Ber. Dtsch. Chem. Ges.* **1903**, *36*, 2382−2384. (b) Ullmann, F.; Bielecki, J. *Ber. Dtsch. Chem. Ges.* **1901**, *34*, 2174−2185.

(2) Goldberg, I. *Ber. Dtsch. Chem. Ges.* **1906**, *39*, 1691−1692.

(3) Hurtley, W. R. H. *J. Chem. Soc.* **1929**, 1870.

(4) (a) Beletskaya, I. P.; Cheprakov, A. V. *Coord. Chem. Rev.* **2004**, *248*, 2337−2364. (b) Evano, G.; Blanchard, N.; Toumi, M. *Chem. Rev.* **2008**, *108*, 3054−3131. (c) Nakamura, E.; Mori, S. *Angew. Chem., Int. Ed.* **2000**, *39*, 3750−3771.

(5) For selected references, see: (a) Allen, S. E.; Walvoord, R. R.; Padilla-Salinas, R.; Kozlowski, M. C. *Chem. Rev.* **2013**, *113*, 6234−6458. (b) Tang, X.; Huang, L.; Xu, Y.; Yang, J.; Wu, W.; Jiang, H. *Angew. Chem., Int. Ed.* **2014**, *53*, 4205−4208. (c) Wang, L.; Yu, X.; Feng, X.; Bao, M. *J. Org. Chem.* **2013**, *78*, 1693−1698. (d) Xu, H.; Man, Q.; Lin, Y.; Li, Y.; Feng, Y. *Chin. J. Org. Chem.* **2010**, *30*, 9−22. (e) Zhang, B.; Wang, Y.; Yang, S.-P.; Zhou, Y.; Wu, W.-B.; Tang, W.; Zuo, J.-P.; Li, Y.; Yue, J.-M. *J. Am. Chem. Soc.* **2012**, *134*, 20605−20608.

(6) (a) Glaser, C. *Ber. Dtsch. Chem. Ges.* **1869**, *2*, 422−424. (b) Hay, A. S. *J. Org. Chem.* **1962**, *27*, 3320−3321. (c) Siemsen, P.; Livingston, R. C.; Diederich, F. *Angew. Chem., Int. Ed.* **2000**, *39*, 2632−2657.

(7) (a) Negishi, E.-i.; Anastasia, L. *Chem. Rev.* **2003**, *103*, 1979−2018. (b) Sonogashira, K. In *Metal-Catalyzed Cross-Coupling Reactions*; Wiley−VCH, 1998; pp 203−229. (c) Sonogashira, K.; Tohda, Y.; Hagihara, N. *Tetrahedron Lett.* **1975**, *16*, 4467−4470.

(8) (a) Batsanov, A. S.; Collings, J. C.; Fairlamb, I. J.; Holland, J. P.; Howard, J. A.; Lin, Z.; Marder, T. B.; Parsons, A. C.; Ward, R. M.; Zhu, J. *J. Org. Chem.* **2005**, *70*, 703−706. (b) Firth, A. G.; Fairlamb, I. J. S.; Darley, K.; Baumann, C. G. *Tetrahedron Lett.* **2006**, *47*, 3529−3533. (c) Shi, W.; Lei, A. *Tetrahedron Lett.* **2014**, *55*, 2763−2772.

(9) (a) Chinchilla, R.; Najera, C. *Chem. Rev.* **2007**, *107*, 874−922. (b) Do, H.-Q.; Daugulis, O. *J. Am. Chem. Soc.* **2009**, *131*, 17052−17053. (c) Hamada, T.; Ye, X.; Stahl, S. S. *J. Am. Chem. Soc.* **2008**, *130*, 833−835. (d) Plenio, H. *Angew. Chem., Int. Ed.* **2008**, *47*, 6954−6956. (e) Punniyamurthy, T.; Rout, L. *Coord. Chem. Rev.* **2008**, *252*, 134−154. (f) Wang, Y.-F.; Deng, W.; Liu, L.; Guo, Q.-X. *Chin. J. Org. Chem.* **2005**, *25*, 8−24.

(10) (a) He, C.; Ke, J.; Xu, H.; Lei, A. *Angew. Chem., Int. Ed.* **2013**, *52*, 1527−1530. (b) Mirica, L. M.; Vance, M.; Rudd, D. J.; Hedman, B.; Hodgson, K. O.; Solomon, E. I.; Stack, T. D. *Science* **2005**, *308*, 1890−1892. (c) Tougerti, A.; Negri, S.; Jutand, A. *Chem. - Eur. J.* **2007**, *13*, 666−676. (d) Vilhelmsen, M. H.; Jensen, J.; Tortzen, C. G.; Nielsen, M. B. *Eur. J. Org. Chem.* **2013**, *2013*, 701−711.

(11) (a) Bai, R.; Zhang, G.; Yi, H.; Huang, Z.; Qi, X.; Liu, C.; Miller, J. T.; Kropf, A. J.; Bunel, E. E.; Lan, Y.; Lei, A. *J. Am. Chem. Soc.* **2014**, *136*, 16760−16763. (b) Bohlmann, F.; Schönowsky, H.; Inhoffen, E.; Grau, G. *Chem. Ber.* **1964**, *97*, 794−800. (c) Zhang, G.; Yi, H.; Zhang, G.; Deng, Y.; Bai, R.; Zhang, H.; Miller, J. T.; Kropf, A. J.; Bunel, E. E.; Lei, A. *J. Am. Chem. Soc.* **2014**, *136*, 924−926.

(12) (a) Fomina, L.; Vazquez, B.; Tkatchouk, E.; Fomine, S. *Tetrahedron* **2002**, *58*, 6741−6747. (b) Jover, J.; Spuhler, P.; Zhao, L.; McArdle, C.; Maseras, F. *Catal. Sci. Technol.* **2014**, *4*, 4200−4209.

(13) (a) Dick, A. R.; Kampf, J. W.; Sanford, M. S. *J. Am. Chem. Soc.* **2005**, *127*, 12790−12791. (b) Gillie, A.; Stille, J. K. *J. Am. Chem. Soc.* **1980**, *102*, 4933−4941. (c) Goldberg, K. I.; Yan, J. Y.; Winter, E. L. *J. Am. Chem. Soc.* **1994**, *116*, 1573−1574. (d) Hartwig, J. F. *Acc. Chem. Res.* **1998**, *31*, 852−860. (e) Moravskiy, A.; Stille, J. K. *J. Am. Chem. Soc.* **1981**, *103*, 4182−4186.

(14) (a) Adams, R. D.; Rassolov, V.; Wong, Y. O. *Angew. Chem.* **2014**, *126*, 11186−11189. (b) Halpern, J. *Inorg. Chim. Acta* **1982**, *62*, 31−37. (c) Powers, D. C.; Ritter, T. *Nat. Chem.* **2009**, *1*, 302−309. (d) Trinquier, G.; Hoffmann, R. *Organometallics* **1984**, *3*, 370−380. (e) Young, S. J.; Kellenberger, B.; Reibenspies, J. H.; Himmel, S. E.; Manning, M.; Anderson, O. P.; Stille, J. K. *J. Am. Chem. Soc.* **1988**, *110*, 5744−5753.

(15) (a) Armentrout, P. B. *Science* **1991**, *251*, 175−179. (b) Poli, R. *Chem. Rev.* **1996**, *96*, 2135−2204. (c) Ling, L.; Liu, K.; Li, X.; Li, Y. *ACS Catal.* **2015**, *5*, 2458−2468.

(16) (a) Carreón-Macedo, J.-L.; Harvey, J. N.; Poli, R. *Eur. J. Inorg. Chem.* **2005**, *2005*, 2999−3008. (b) Agenet, N.; Gandon, V.; Vollhardt, K. P.; Malacria, M.; Aubert, C. *J. Am. Chem. Soc.* **2007**, *129*, 8860−8871. (c) Popp, B. V.; Stahl, S. S. *Chem. - Eur. J.* **2009**, *15*, 2915−2922. (d) Dahy, A. A.; Koga, N. *J. Organomet. Chem.* **2010**, *695*, 2240−2250. (e) Cheng, G.-J.; Song, L.-J.; Yang, Y.-F.; Zhang, X.; Wiest, O.; Wu, Y.-D. *ChemPlusChem* **2013**, *78*, 943−951. (f) Yu, H.; Fu, Y.; Guo, Q.; Lin, Z. *Organometallics* **2009**, *28*, 4443−4451.

(17) (a) Fiedler, A.; Schroeder, D.; Shaik, S.; Schwarz, H. *J. Am. Chem. Soc.* **1994**, *116*, 10734−10741. (b) Schröder, D.; Shaik, S.; Schwarz, H. *Acc. Chem. Res.* **2000**, *33*, 139−145. (c) Harvey, J. N.; Poli, R.; Smith, K. M. *Coord. Chem. Rev.* **2003**, *238*−*239*, 347−361.

DOI: 10.1021/acs.joc.5b02797
J. Org. Chem. 2016, 81, 1654−1660

(18) (a) Koga, N.; Morokuma, K. *Chem. Phys. Lett.* **1985**, *119*, 371−374. (b) Lundberg, M.; Siegbahn, P. E. M. *Chem. Phys. Lett.* **2005**, *401*, 347−351. (c) Stranger, R.; Yates, B. F. *Chem. Phys.* **2006**, *324*, 202−209.
(19) (a) Lin, Z. *Acc. Chem. Res.* **2010**, *43*, 602−611. (b) Garcia-Melchor, M.; Braga, A. A.; Lledos, A.; Ujaque, G.; Maseras, F. *Acc. Chem. Res.* **2013**, *46*, 2626−2634. (c) Yang, Y.-F.; Cheng, G.-J.; Liu, P.; Leow, D.; Sun, T.-Y.; Chen, P.; Zhang, X.; Yu, J.-Q.; Wu, Y.-D.; Houk, K. N. *J. Am. Chem. Soc.* **2014**, *136*, 344−355.
(20) (a) Braga, A. A.; Morgon, N. H.; Ujaque, G.; Maseras, F. *J. Am. Chem. Soc.* **2005**, *127*, 9298−9307. (b) Giri, R.; Lan, Y.; Liu, P.; Houk, K. N.; Yu, J.-Q. *J. Am. Chem. Soc.* **2012**, *134*, 14118−14126.
(21) (a) Fuentes, B.; García-Melchor, M.; Lledós, A.; Maseras, F.; Casares, J. A.; Ujaque, G.; Espinet, P. *Chem. - Eur. J.* **2010**, *16*, 8596−8599. (b) Gellrich, U.; Meissner, A.; Steffani, A.; Kahny, M.; Drexler, H. J.; Heller, D.; Plattner, D. A.; Breit, B. *J. Am. Chem. Soc.* **2014**, *136*, 1097−1104. (c) Liu, Q.; Lan, Y.; Liu, J.; Li, G.; Wu, Y. D.; Lei, A. *J. Am. Chem. Soc.* **2009**, *131*, 10201−10210. (d) Mollar, C.; Besora, M.; Maseras, F.; Asensio, G.; Medio-Simón, M. *Chem. - Eur. J.* **2010**, *16*, 13390−13397. (e) Williams, V. M.; Kong, J. R.; Ko, B. J.; Mantri, Y.; Brodbelt, J. S.; Baik, M. H.; Krische, M. J. *J. Am. Chem. Soc.* **2009**, *131*, 16054−16062.
(22) Frisch, M. J. *Gaussian 09, Revision D.01*, Gaussian, Inc., Wallingford, CT, 2013. The full author list is shown in the Supporting Information..
(23) (a) Becke, A. D. *J. Chem. Phys.* **1993**, *98*, 5648−5652. (b) Lee, C.; Yang, W.; Parr, R. G. *Phys. Rev. B: Condens. Matter Mater. Phys.* **1988**, *37*, 785.
(24) (a) Dolg, M.; Stoll, H.; Preuss, H. *J. Chem. Phys.* **1989**, *90*, 1730. (b) Dolg, M.; Wedig, U.; Stoll, H.; Preuss, H. *J. Chem. Phys.* **1987**, *86*, 866.
(25) Marenich, A. V.; Cramer, C. J.; Truhlar, D. G. *J. Phys. Chem. B* **2009**, *113*, 6378−6396.
(26) (a) Peverati, R.; Truhlar, D. G. *J. Phys. Chem. Lett.* **2012**, *3*, 117−124. (b) Peverati, R.; Truhlar, D. G. *Phys. Chem. Chem. Phys.* **2012**, *14*, 11363−11370. (c) Zhao, Y.; Ng, H. T.; Peverati, R.; Truhlar, D. G. *J. Chem. Theory Comput.* **2012**, *8*, 2824−2834. (d) Liu, D.; Tang, S.; Yi, H.; Liu, C.; Qi, X.; Lan, Y.; Lei, A. *Chem. - Eur. J.* **2014**, *20*, 15605−15610. (e) Qi, X.; Zhang, H.; Shao, A.; Zhu, L.; Xu, T.; Gao, M.; Liu, C.; Lan, Y. *ACS Catal.* **2015**, *5*, 6640−6647.
(27) (a) Harvey, J. N.; Aschi, M.; Schwarz, H.; Koch, W. *Theor. Chem. Acc.* **1998**, *99*, 95−99. (b) Harvey, J. N.; Aschi, M. *Phys. Chem. Chem. Phys.* **1999**, *1*, 5555−5563. (c) Poli, R.; Harvey, J. N. *Chem. Soc. Rev.* **2003**, *32*, 1−8.
(28) Legault, C. Y. *CYLView, 1.0b*; Université de Sherbrooke, Canada, 2009; http://www.cylview.org.
(29) Actually, the 1,1-reductive elimination occurring from a Cu(III) acetylide complex was also considered in this work. The generation of Cu(III) acetylide complex **28b** from singlet Cu dimer **28** is endergonic by 14.9 kcal/mol, which indicates the formation of Cu(III) acetylide complex is energetically unfavorable. The Cu(III) mechanism for C−C bond formation is thereby excluded. Computational details can be found in Figure S2.
(30) Besides the singlet state and triplet state, the singlet diradical state intermediates for C−C bond formation are also calculated. However, the obtained structures are all singlets after many attempts. The singlet diradical state complex cannot be located in this work. See Figures S4 and S5 in the Supporting Information for details.
(31) To verify that this energy span is compatible with the experimental temperature, a DFT study is cited for reference: (a) Kresze, G.; Schulz, G. *Tetrahedron* **1961**, *12*, 7−12. (b) Levandowski, B. J.; Houk, K. N. *J. Org. Chem.* **2015**, *80*, 3530−3537.

DOI: 10.1021/acs.joc.5b02797
J. Org. Chem. 2016, 81, 1654−1660